

Published in final edited form as:

*Tetrahedron Lett.* 2008 October 13; 49(42): 6050–6053. doi:10.1016/j.tetlet.2008.07.178.

## Structure determination and absolute configuration of cannabichromanone derivatives from high potency *Cannabis sativa*

Safwat A. Ahmed<sup>a</sup>, Samir A. Ross<sup>a,b,\*</sup>, Desmond Slade<sup>a</sup>, Mohamed M. Radwan<sup>a</sup>, Ikhlas A. Khan<sup>a,b</sup>, and Mahmoud A. ElSohly<sup>a,c,\*</sup>

<sup>a</sup>National Center for Natural Products Research, School of Pharmacy, The University of Mississippi, University, Mississippi 38677, USA

<sup>b</sup>Department of Pharmacognosy, School of Pharmacy, The University of Mississippi, University, Mississippi 38677, USA

<sup>c</sup>Department of Pharmaceutics, School of Pharmacy, The University of Mississippi, University, Mississippi 38677, USA

### Abstract

Three new cannabichromanone derivatives were isolated from high potency cannabis, along with the known cannabichromanone. Full spectroscopic data, including the use of electronic circular dichroism and Mosher ester analysis to determine the absolute configuration of these compounds, are reported. All isolates were tested for antimicrobial, antimalarial, antileishmanial and anti-oxidant activity.

### Keywords

*Cannabis sativa*; Absolute configuration; Cannabichromanone; Circular dichroism; Mosher ester analysis; Antimicrobial; Antimalarial; Antileishmanial; Anti-oxidant

*Cannabis sativa* L. is one of the oldest medicinal plants known, having been used for more than five thousand years.<sup>1</sup> Cannabis has an extremely complex and diverse chemistry due to the vast number of its constituents and their possible interaction with one another.<sup>2–3</sup> Phytocannabinoids are unique to cannabis and are responsible for a wide range of biological activities including analgesic,<sup>4</sup> anti-emetic,<sup>5</sup> antidepressant,<sup>6</sup> appetite stimulation,<sup>7</sup> anticancer,<sup>8</sup> glaucoma treatment<sup>9</sup> and psychoactivity.<sup>10</sup>

As part of our phytochemical investigation<sup>11–13</sup> of high potency cannabis<sup>14</sup> ( $\Delta^9$ -THC > 10% by dry weight), we herein report the isolation of three new cannabichromanone derivatives (2–4) (Figure 1) and the known cannabichromanone (1), including the first report of the full

© 2008 Elsevier Ltd. All rights reserved.

\*Corresponding authors. Tel.: +1-662-915-5928; fax: +1-662-915-5587; e-mail: melsohly@olemiss.edu (M.A. ElSohly). Tel.: +1-662-915-1031; fax: +1-662-915-7989; e-mail: sross@olemiss.edu (S.A. Ross).

**Publisher's Disclaimer:** This is a PDF file of an unedited manuscript that has been accepted for publication. As a service to our customers we are providing this early version of the manuscript. The manuscript will undergo copyediting, typesetting, and review of the resulting proof before it is published in its final citable form. Please note that during the production process errors may be discovered which could affect the content, and all legal disclaimers that apply to the journal pertain.

spectroscopic data and absolute configuration for **1**. All compounds were evaluated for antimicrobial,<sup>15</sup> antimalarial,<sup>16</sup> antileishmanial<sup>11,17</sup> and anti-oxidant activity.<sup>18</sup>

Whole buds of mature female plants grown from high potency Mexican seeds were processed and stored at low temperature ( $-24^{\circ}\text{C}$ ). The material was authenticated by Dr. Suman Chandra, The University of Mississippi, and a voucher specimen (S1310V1) was deposited at the Coy Waller Complex, The University of Mississippi.

Plant material (9.0 kg, *ca.* 10% THC) was sequentially extracted at room temperature [hexanes ( $2 \times 60$  L),  $\text{CH}_2\text{Cl}_2$  (48 L), EtOAc (40 L), EtOH (37.5 L), EtOH/ $\text{H}_2\text{O}$  (36 L, 1:1) and  $\text{H}_2\text{O}$  (40 L)] and the extracts concentrated under reduced pressure at  $40^{\circ}\text{C}$ . The hexanes extract (0.96 kg) was subjected to vacuum liquid chromatography (VLC) on flash silica gel eluting with hexanes, EtOAc and MeOH gradient. The hexanes/EtOAc (50:50) fraction was subjected to column chromatography and final purification by semi-preparative C18 HPLC (MeCN/ $\text{H}_2\text{O}$ , 75:25) afforded **1** (15 mg,  $R_t = 14$  min), **2** (30 mg,  $R_t = 10$  min), **3** (4 mg,  $R_t = 8$  min) and **4** (60 mg,  $R_t = 8.5$  min).

Compound **1** was obtained as a yellow oil  $\{[\alpha]_D^{25} -25.19$  (*c* 0.5,  $\text{CHCl}_3$ ) $\}$  and its molecular formula was determined to be  $\text{C}_{20}\text{H}_{28}\text{O}_4$  by HRESIMS [ $m/z$  calcd for  $\text{C}_{20}\text{H}_{28}\text{O}_4\text{Na}$ : 355.1885 ( $\text{M}+\text{Na}$ ) $^+$ , found 355.1901], representing seven degrees of unsaturation. The IR spectrum exhibited hydroxyl and conjugated carbonyl absorption bands at 3346 and  $1632\text{ cm}^{-1}$ , respectively. The  $^{13}\text{C}$ -NMR, DEPT-135 and HMQC spectra of **1** revealed the presence of 20 carbon resonances, including four methyl, six methylene, three methine and seven quaternary carbons [two oxyaryl (C-1, C-4a), two carbonyl (C-8, C-3''), IR absorption at 1632 and  $1730\text{ cm}^{-1}$ , respectively), two aryl  $\text{sp}^2$  (C-3, C-8a) and one oxygenated  $\text{sp}^3$  (C-6) carbon]. The  $^1\text{H}$ -NMR spectrum of **1** (Table 1) showed two aromatic protons at  $\delta_{\text{H}}$  6.18 (s, H-2) and 6.26 (s, H-4), four methyl signals at  $\delta_{\text{H}}$  0.86 (t, H-5'), 1.38 (s, H-9), 1.43 (s, H-10) and 2.12 (s, H-4''), six methylenes at  $\delta_{\text{H}}$  2.47 (t, H-1'), 1.56 (m, H-2'), 1.28 (m, H-3' and H-4'), 2.00 (m, H-1'') and 2.59 (m, H-2''), one methine at  $\delta_{\text{H}}$  2.40 (dd, H-7) and a sharp singlet at  $\delta_{\text{H}}$  11.52 (Ar-OH). The downfield shift of this phenolic proton compared to the usual range of 5–8 ppm is due to hydrogen bonding with the C-8 carbonyl oxygen and was further confirmed by HMBC correlations with C-1, C-2 and C-8a (Figure 2). Detailed 2D NMR and UV ( $\lambda_{\text{max}}$  at 210, 279 and 350 nm)<sup>19</sup> experiments confirmed the presence of a 4-chromanone ring system with hydroxyl group at C-1, *n*-pentyl moiety at C-3, dimethyl at C-6 and 3''-oxobutyl moiety at C-7 (Figure 2), establishing **1** as cannabichromanone A<sup>20</sup> (Figure 1) [name based on 4-chromanone system: 5-hydroxy-2,2-dimethyl-3-(3-oxobutyl)-7-*n*-pentylchroman-4-one<sup>21</sup>].

Compound **2** was obtained as a yellow oil  $\{[\alpha]_D^{25} -19.81$  (*c* 0.5,  $\text{CHCl}_3$ ) $\}$  and its molecular formula was determined to be  $\text{C}_{21}\text{H}_{30}\text{O}_5$  by HRESIMS [ $m/z$  calcd for  $\text{C}_{21}\text{H}_{31}\text{O}_5$ : 363.2171 ( $\text{M}+\text{H}$ ) $^+$ , found 363.2052], representing seven degrees of unsaturation. Compound **2** has the same basic structure as **1**, with the exception of an additional hydroxymethine functionality [ $\delta_{\text{H}}$  4.20 (m, H-1''),  $\delta_{\text{C}}$  73.2 (C-1'')] established by COSY correlations (H-7/H-1'', H-1''/H-2'') and HMBC (H-1''/C-6, C-2'', C-3'' and C-8), confirming **2** as cannabichromanone B (Figure 1) [name based on 4-chromanone system: 5-hydroxy-3-(1-hydroxy-4-oxopentyl)-2,2-dimethyl-7-*n*-pentylchroman-4-one<sup>21</sup>].

Compound **3** was obtained as a yellow oil  $\{[\alpha]_D^{25} +7.99$  (*c* 0.01,  $\text{CHCl}_3$ ) $\}$  and its molecular formula was determined to be  $\text{C}_{21}\text{H}_{28}\text{O}_5$  by HRESIMS [ $m/z$  calcd for  $\text{C}_{21}\text{H}_{28}\text{O}_5\text{Na}$ : 383.1834 ( $\text{M}+\text{Na}$ ) $^+$ , found 383.1838], representing eight degrees of unsaturation. Compound **3** has the same basic structure as **1** and **2**, except for an additional carbonyl moiety [ $\delta_{\text{C}}$  207.7 (C-4'')] established by HMBC (H<sub>2</sub>-1''/C-3'', H<sub>3</sub>-5''/C-3'', C-4''), confirming **3** as cannabichromanone C (Figure 1) [name based on 4-chromanone system: 5-hydroxy-2,2-dimethyl-3-(3,4-dioxopentyl)-7-*n*-pentylchroman-4-one<sup>21</sup>].

Compound **4** was obtained as a yellow oil  $\{[\alpha]_D^{25} -14.13 (c 0.5, \text{CHCl}_3)\}$  and its molecular formula was determined to be  $\text{C}_{21}\text{H}_{28}\text{O}_3$  by HRESIMS [ $m/z$  calcd for  $\text{C}_{21}\text{H}_{27}\text{O}_3$ : 329. 2117 ( $\text{M}+\text{H}$ )<sup>+</sup>, found 329.2089], representing eight degrees of unsaturation. The  $^{13}\text{C}$ -NMR spectrum showed signals indicating four methyl, six methylene, four methine and seven quaternary carbons [two oxyaryl (C-1, C-4a), one carbonyl (C-8, IR absorption at  $1730\text{ cm}^{-1}$ ), two aryl  $\text{sp}^2$  (C-3, C-8a), one oxygenated  $\text{sp}^2$  (C-4'') and one oxygenated  $\text{sp}^3$  (C-6) carbon]. The  $^1\text{H}$ -NMR spectrum of **4** (Table 1) showed two aromatic protons at  $\delta_{\text{H}}$  6.52 (s, H-2) and 6.34 (s, H-4), one olefinic proton at  $\delta_{\text{H}}$  5.91 (br s, H-3''), four methyl signals at  $\delta_{\text{H}}$  0.84 (t, H-5'), 1.15 (s, H-9), 1.41 (s, H-10) and 1.94 (s, H-5''), six methylenes at  $\delta_{\text{H}}$  2.42 (t, H-1'), 1.52 (m, H-2'), 1.27 (m, H-3', H-4'), 1.38 (m, H-1'') and 2.36 (m, H-2''), and one methine at  $\delta_{\text{H}}$  2.65 (dd, H-7). HMBC and COSY experiments (Figure 2) confirmed the presence of a substituted 4-chromanone system with UV absorption maxima  $\lambda_{\text{max}}$  209, 279 and 350 nm. The absence of a chelated hydroxyl proton at *ca.*  $\delta_{\text{H}}$  11.5, the upfield shift of C-1 to  $\delta_{\text{C}}$  144.8, the molecular formula, degrees of unsaturation and 2D NMR analysis (Figure 2) pointed towards an oxygen-bridge between C-4'' and C-1, resulting in a rare nine membered ring.<sup>22–23</sup> The geometry of the  $\Delta^{3,4''}$  system was assigned as *Z* on the basis of ROESY correlations between H-3'' and H<sub>3</sub>-5'', establishing **4** as cannabichromanone D (Figure 1) [name based on 4-chromanone system: 2,2-dimethyl-3,5-(4-yloxy-pent-3-en-1-yl)-7-*n*-pentylchroman-4-one<sup>21</sup>].

Conformational analysis of **3** indicated the sofa conformation (E-conformer), with the pentane-3'',4''-dione group at C-7 in the pseudoequatorial position and the two methyls at C-6 in the equatorial and axial positions, as the lowest energy conformer (Figure 3). This was confirmed by ROESY analysis indicating correlation between H<sub>ax</sub>-7 [ $\delta_{\text{H}}$  3.12 (d)] and H<sub>3</sub>-10 [ $\delta_{\text{H}}$  1.46 (s),  $\delta_{\text{C}}$  26.0 (equatorial)], while no correlation was observed between H<sub>ax</sub>-7 [ $\delta_{\text{H}}$  3.12 (d)] and H<sub>3</sub>-9 [ $\delta_{\text{H}}$  1.38 (s),  $\delta_{\text{C}}$  23.3 (axial)]. Correlation between H<sub>ax</sub>-7 and both H<sub>3</sub>-9 and H<sub>3</sub>-10 would suggest an unfavorable C-6/C-7 *trans*-diaxial configuration.

Optical rotatory dispersion (ORD) and electronic circular dichroism (CD) have been used to determine the absolute configuration and conformation of natural products, e.g. flavonoids,<sup>24</sup> and in qualitative analysis of THC and CBD content.<sup>25</sup> The modified octant rule,<sup>26</sup> defining the relationship between the chirality of  $\alpha,\beta$ -unsaturated ketones and the sign of their high wavelength Cotton effect (CE), was extended to aryl ketones or acetophenones.<sup>27</sup> Compound **3** shows UV absorption at 279 nm ( $\pi \rightarrow \pi^*$ ) and 350 nm ( $n \rightarrow \pi^*$ ) and applying the octant rule modified for cyclic arylketones, a positive CE for the  $n \rightarrow \pi^*$  carbonyl transition would indicate *7R* and a negative CE for the  $n \rightarrow \pi^*$  carbonyl transition would indicate *7S* absolute configuration.<sup>24</sup> A positive CE at 313 nm (0.2 mg/ml, MeOH) was observed for **3** (Figure 4), establishing the absolute configuration as *7R*. Conversely, **1**, **2** and **4** displayed negative CE at the  $n \rightarrow \pi^*$  carbonyl transition (320–350 nm), indicating *7S* absolute configuration for these compounds (Table 2).

The absolute configuration of **2** at the secondary carbinol chiral center (C-1'') was determined via the Mosher ester analysis protocol.<sup>28–31</sup> This protocol involves derivatization of the carbinol with each of the enantiomeric pair (*R*)-(-)-MTPA-Cl and (*S*)-(+)-MTPA-Cl ( $\alpha$ -methoxy- $\alpha$ -trifluoromethylphenylacetyl chloride) giving two diastereoisomeric esters [(*S*)- and (*R*)-ester, respectively]. NMR analysis of each of the two esters can be used to determine the absolute configuration of the chiral center. The NMR analysis is based on an empirical conformation for the esters that dictate the spectroscopic features of the conformers. This conformation includes an *s-trans* (antiperiplanar) arrangement about the O-CO bond and a *syn*-coplanar ( $0^\circ$  dihedral angle) arrangement between of the  $\text{CF}_3$  group and the carbinol methine proton with respect to the carbonyl group (Figure 5). The MTPA aryl substituent causes an anisotropic, magnetic shielding effect on protons above or below the plane of the aryl ring, resulting in an upfield chemical shift for the spatially proximal protons in the NMR spectrum. This implies that protons in the  $\text{R}^2$ -group of the (*S*)-ester are more shielded and hence

upfield. The same applies for protons in the R<sup>1</sup>-group of the (R)-ester. The sign of  $\Delta\delta_{\text{H}}(\text{SR}) = \delta_{\text{H}}(\text{S}) - \delta_{\text{H}}(\text{R})$  for protons in R<sup>1</sup> will therefore be positive and for protons in R<sup>2</sup> negative, yielding the absolute configuration of the secondary carbinol chiral center. The (S)- and (R)-MRPA-esters for **2** were prepared as follows: In a NMR tube **2** (2 mg) in pyridine-d<sub>5</sub> (100  $\mu$ l) was reacted with (R)-(-)-MTPA-Cl (30  $\mu$ l) at room temperature (2 hours) to afford (2S)-ester. Similarly, (2R)-ester was prepared from (S)-(+)-MTPA-Cl. <sup>1</sup>H-NMR data was measured directly from the reaction mixtures (Table 3). A negative  $\Delta\delta_{\text{H}}(\text{SR})$  for H-7 indicates aryl-shielding of the C-7 moiety in the (S)-ester and therefore 1<sup>o</sup>R absolute configuration, establishing **2** as 5-hydroxy-3S-(1R-hydroxy-4-oxopentyl)-2,2-dimethyl-7-n-pentylchroman-4-one.

The isolated compounds were evaluated for antimicrobial (*Candida albicans* ATCC 90028, *Escherichia coli* ATCC 35218, *Pseudomonas aeruginosa* ATCC 27853, *Mycobacterium intracellulare* ATCC 23068, *Aspergillus fumigat* ATCC 90906 and Methicillin Resistant *Staphylococcus aureus* ATCC 43300), antimalarial [*Plasmodium falciparum* (chloroquine sensitive D6 clone) and *P. falciparum* (chloroquine resistant W2 clone)], antileishmanial and anti-oxidant activity.

The isolated compounds showed no antimicrobial activity. Compounds **1** and **3** showed mild antimalarial activity against *P. falciparum* (D6 and W2 clone) with IC<sub>50</sub> values of 3.7 and 3.8  $\mu$ g/mL, and 4.7 and 3.4  $\mu$ g/mL, respectively. Compounds **2** and **4** displayed no antimalarial activity. Compounds **1–4** showed moderate antileishmanial activity with IC<sub>50</sub> values of 14.0, 14.0, 12.5 and 9.0  $\mu$ g/mL, respectively.

A TLC autographic assay for 1,1-diphenyl-2-picrylhydrazyl (DPPH) radical-scavenging effect was used to determine anti-oxidant activity. The isolated compounds were dissolved in DMF (2 mg/mL) and applied in the form of a spot (4  $\mu$ l, 4–5 mm in diameter) on silica gel GF plates. The residual DMF was removed under vacuum (15–20 min). A similar amount of vitamin E in DMF was used as positive anti-oxidant control. The radical-scavenging effects of the compounds were detected on the TLC plate using DPPH spray reagent (0.2% w/v in methanol). The plate was observed 30 min after spraying. Active compounds are observed as yellow spots against a purple background. Relative radical-scavenging activity was assigned as “strong” (compounds that produce an intense bright yellow spot), “medium” (compounds that produce a clear yellow spot), “weak” (compounds that produce a weakly visible yellow spot), or “not active” (compounds that produce no yellow spot).<sup>32</sup> Vitamin E produced an intense bright yellow spot. The isolated compounds all produced a bright yellow spot, indicating “strong” anti-oxidant activity.

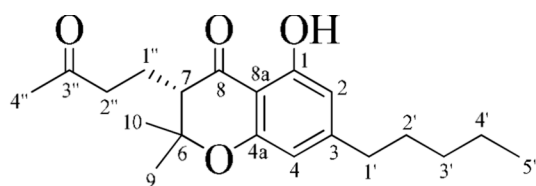
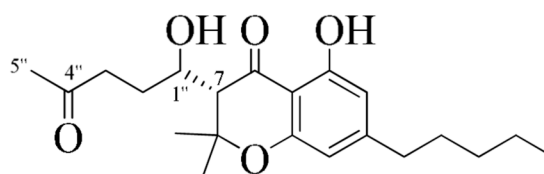
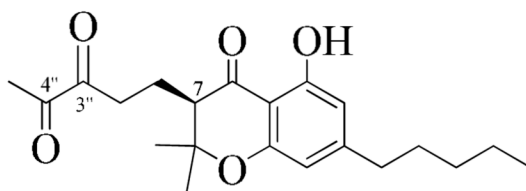
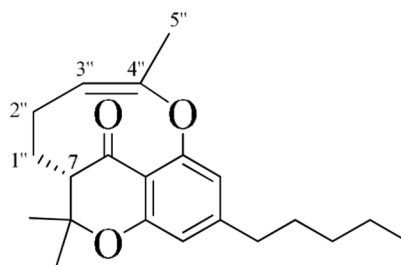
## Acknowledgment

The project described was supported in part by Grant Number 5P20RR021929-02 from the National Center for Research Resources and in part by the National Institute on Drug Abuse, contract # N01DA-5-7746. The content is solely the responsibility of the authors and does not necessarily represent the official views of the National Center for Research Resources or the National Institutes of Health. We are grateful to Dr. Bharathi Avula for assistance with the HRESIMS, and to Dr. Melissa Jacob, Ms. Marsha Wright, Dr. Shabana Khan and Dr. Babu Tekwani for conducting the antimicrobial, antimalarial and antileishmanial testing.

## References and notes

1. Fransworth NR. J. Am. Pharm. Assoc 1969;9:410–414. [PubMed: 5799730]
2. ElSohly MA, Slade D. Life Sci 2005;78:539–548. [PubMed: 16199061]
3. Brenneisen, R. Chapter 2 – Chemistry and Analysis of Phytocannabinoids and Other Cannabis Constituents. In: ElSohly, MA., editor. Marijuana and the Cannabinoids. Totowa, New Jersey: Humana Press Inc; 2007. p. 17-50.

4. Roberts JD, Gennings C, Shih M. *Eur. J. Pharmacol* 2006;530:54–58. [PubMed: 16375890]
5. Darmani NA, Johnson JC. *Eur. J. Pharmacol* 2004;488:201–212. [PubMed: 15044052]
6. Moreira FA. *J. Neurosci* 2007;27:13369–13370. [PubMed: 18057193]
7. Wilson MMG, Philpot C, Morley JE. *J. Nutr. Health Aging* 2007;11:195–198. [PubMed: 17435963]
8. Blazquez C, Carracedo A, Salazar M, Lorente M, Egia A, Gonzalez-Feria L, Haro A, Velasco G, Guzman M. *Neuropharmacology* 2008;54:235–243. [PubMed: 17675107]
9. Plange N, Arend KO, Kaup M, Doehmen B, Adams H, Hendricks S, Cordes A, Huth J, Sponsel WE, Remky A. *Am. J. Ophthalmol* 2007;143:173–174. [PubMed: 17188063]
10. Gomez-Ruiz M, Hernandez M, de Miguel R, Ramos JA. *Mol. Neurobiol* 2007;36:3–14. [PubMed: 17952645]
11. Radwan MM, Ross SA, Slade D, Ahmed SA, Zulfiqar F, ElSohly MA. *Planta Med* 2008;74:267–272. [PubMed: 18283614]
12. Ahmed SA, Ross SA, Slade D, Radwan MM, Zulfiqar F, ElSohly MA. *J. Nat. Prod* 2008;71:536–542. [PubMed: 18303850]
13. Radwan MM, ElSohly MA, Slade D, Ahmed SA, Wilson L, El-Alfy AT, Khan IA, Ross SA. *Phytochemistry*. 2008submitted.
14. ElSohly MA, Ross SA, Mehmedic Z, Arafat R, Yi B, Banahan BF. *J. Forensic Sci* 2000;45:24–30. [PubMed: 10641915]
15. Bharate SB, Khan SI, Yunus NAM, Chauthe SK, Jacob MR, Tekwani BL, Khan IA, Singh IP. *Bioorg. Med. Chem* 2007;15:87–96. [PubMed: 17070063]
16. Howlett AC, Barth F, Bonner TI, Cabral G, Casellas P, Devane WA, Felder CC, Herkenham M, Mackie K, Martin BR, Mechoulam R, Pertwee RG. *Pharmacol. Rev* 2002;54:161–202. [PubMed: 12037135]
17. Rocha LG, Almeida JRGS, Macedo RO, Barbosa-Filho JM. *Phytomedicine* 2005;12:514–535. [PubMed: 16008131]
18. Hampson AJ, Grimaldi M, Lolic M, Wink D, Rosenthal R, Axelrod J. *Ann. N. Y. Acad. Sci* 2000;899:274–282. [PubMed: 10863546]
19. Rukachaisirikul V, Chantaruk S, Pongcharoen W, Isaka M, Lapanun S. *J. Nat. Prod* 2006;69:980–982. [PubMed: 16792425]
20. Friedrich-Fiechtel J, Spiteller G. *Tetrahedron* 1975;31:479–487.
21. See reference <sup>2</sup> for cannabinoid numbering system.
22. Glaser R, Shiftan D. *Adv. Mol. Struct. Res* 1999;5:89–151.
23. Holmes, AB.; McGeary, RP. *Comprehensive Heterocyclic Chemistry II: Volume 9: Seven-Membered and Larger Rings and All Fused Derivatives*. Newkome, GR., editor. Oxford, UK: Elsevier Science Ltd; 1996. p. 737-788.p. 1039-1146.Nine-membered rings,
24. Slade D, Ferreira D, Marais JPI. *Phytochemistry* 2005;66:2177–2215. [PubMed: 16153414]
25. Han SM, Purdie N. *Anal. Chem* 1985;57:2068–2071.
26. Snatzke G. *Tetrahedron* 1965;21:413–419.
27. Snatzke G. *Tetrahedron* 1965;21:439–448.
28. Dale JA, Mosher HS. *J. Am. Chem. Soc* 1973;95:512–519.
29. Sullivan GR, Dale JA, Mosher HS. *J. Org. Chem* 1973;38:2143–2147.
30. Hoye TR, Jeffrey CS, Shao F. *Nat. Protoc* 2007;2:2451–2458. [PubMed: 17947986]
31. Seco JM, Quinoa E, Riguera R. *Chem. Rev* 2004;104:17–117.
32. Takamatsu S, Hodges TW, Rajbhandari I, Gerwick WH, Hamann MT, Nagle DG. *J. Nat. Prod* 2003;66:605–608. [PubMed: 12762791]

**1****2****3****4**

**Figure 1.** Cannabichromanone derivatives **1–4** with cannabinoid numbering system.<sup>21</sup>

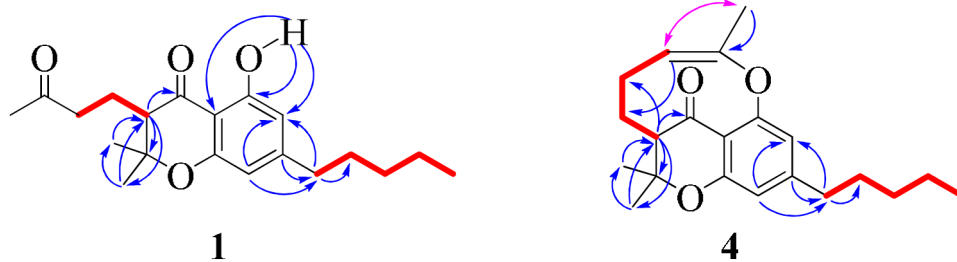


**Figure 2.** Important HMBC (blue arrows), COSY (red bold) and ROESY (purple double-faced arrow) correlations of **1** and **4**.

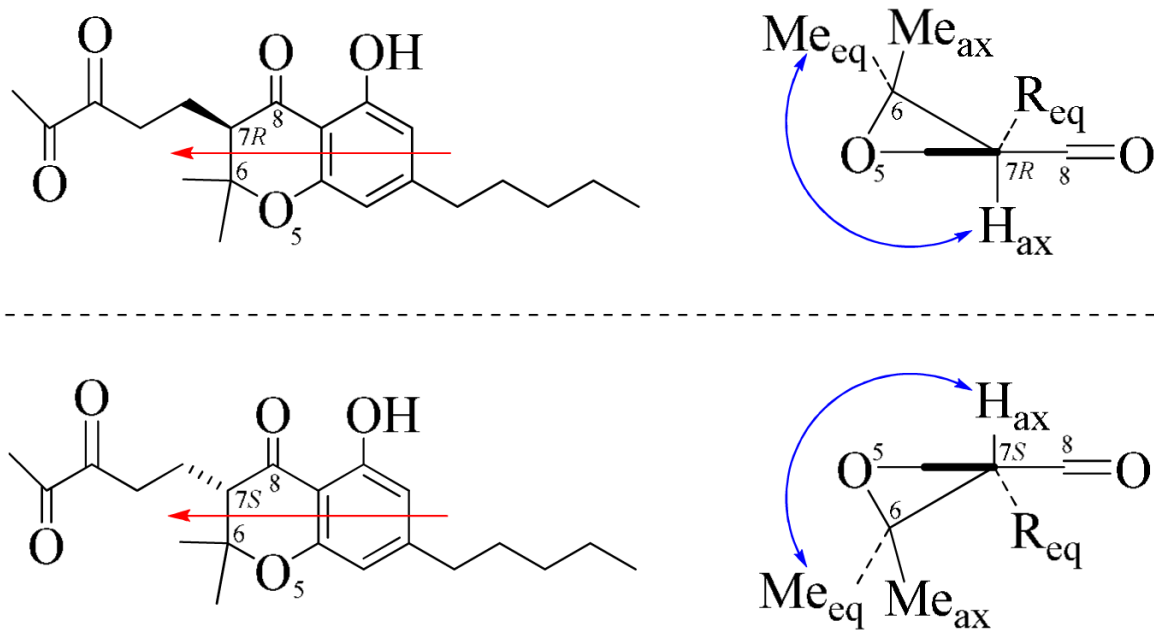


**Figure 3.** Conformational analysis for **3**. The red arrow indicates the direction of projection. The back wedge represents the plane of the benzenoid ring. The blue arrow indicates ROESY correlation between H<sub>3-9</sub> or H<sub>3-10</sub> and H-7.



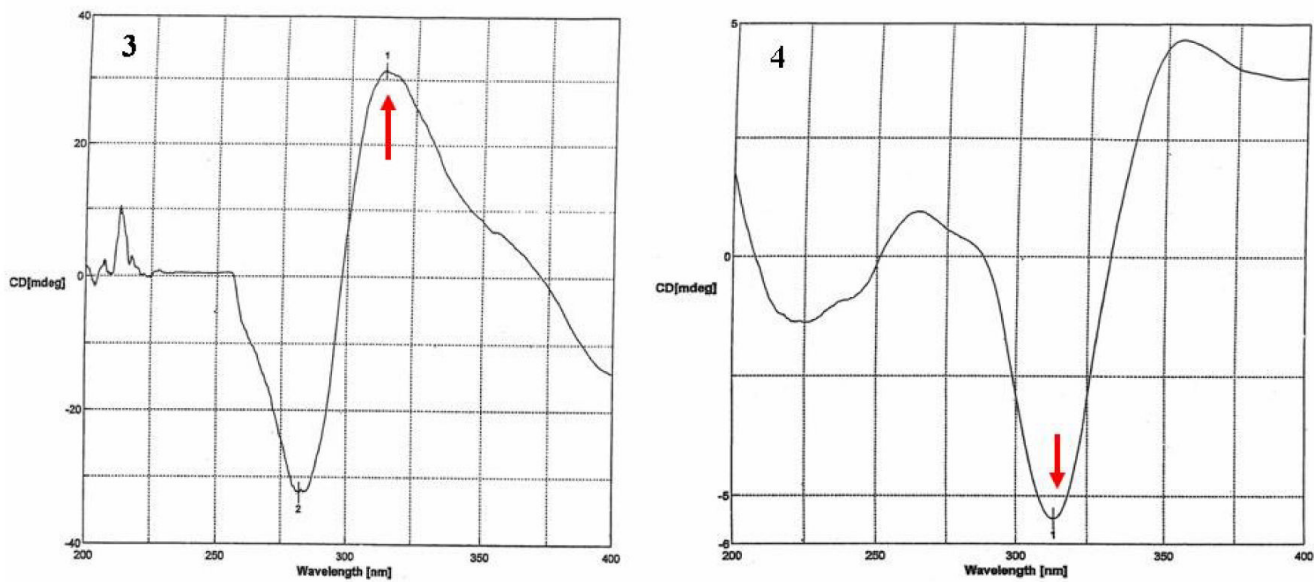


**Figure 4.**  
CD spectra for 3 and 4.

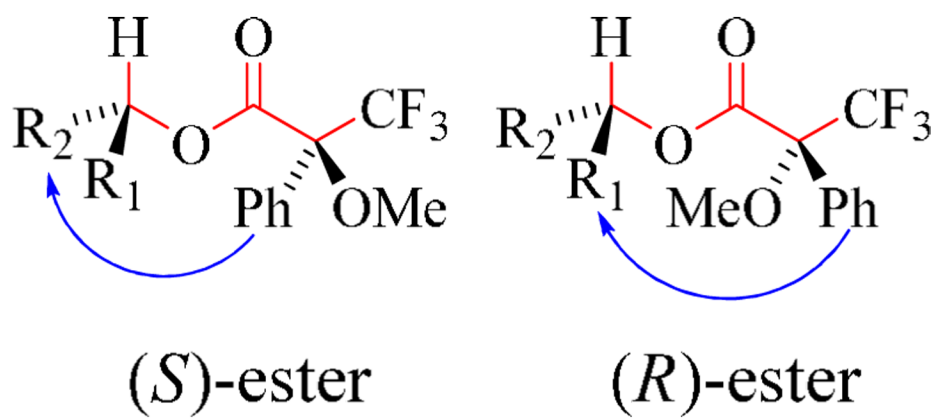


**Figure 5.** Conformation of (*S*)- and (*R*)-esters. The atoms and bonds in red are coplanar. The blue arrow indicates the phenyl shielding effect

**Table 1**  
 $^1\text{H}$ - and  $^{13}\text{C}$ -NMR data of **1–4** in  $\text{CDCl}_3$  (500 MHz for  $^1\text{H}$ , 100 MHz for  $^{13}\text{C}$ )<sup>a</sup>

No	1		2		3		4	
	$\delta_{\text{C}}$	$\delta_{\text{H}}$ (mult, $J$ )	$\delta_{\text{C}}$	$\delta_{\text{H}}$ (mult, $J$ )	$\delta_{\text{C}}$	$\delta_{\text{H}}$ (mult, $J$ )	$\delta_{\text{C}}$	$\delta_{\text{H}}$ (mult, $J$ )
1	161.8		161.8		163.9		144.8	
2	107.9	6.18 (s)	108.0	6.17 (s)	114.4	6.66 (s)	111.4	6.52 (s)
3	155.5		155.7		156.3		133.1	
4	108.7	6.26 (s)	108.8	6.25 (s)	117.0	6.42 (s)	116.2	6.34 (s)
4a	159.3		159.3		156.3		140.7	
6	81.5		81.4		82.6		82.6	
7	53.6	2.40 (dd, 10.8)	53.4	2.40 (d, 6.4)	55.9	3.12 (d, 10.4)	54.5	2.65 (dd, 4.0, 14.0)
8	201.1		200.9		198.8		202.0	
8a	105.0		105.0		112.6		137.6	
9	23.4	1.38 (s)	23.6	1.36 (s)	23.3	1.38 (s)	20.7	1.15 (s)
10	26.6	1.43 (s)	26.4	1.41 (s)	26.0	1.46 (s)	26.8	1.41 (s)
1'	36.9	2.47 (t, 7.2)	36.9	2.47 (t, 7.2)	36.7	2.58 (t, 7.2)	35.7	2.42 (t, 7.2)
2'	30.3	1.56 (m)	30.2	1.56 (m)	30.3	1.60 (m)	31.5	1.52 (m)
3'	31.6	1.28 (m)	31.6	1.28 (m)	31.5	1.32 (m)	31.6	1.27 (m)
4'	22.7	1.28 (m)	22.7	1.28 (m)	22.7	1.32 (m)	22.8	1.27 (m)
5'	14.2	0.86 (t, 6.4)	14.2	0.84 (t, 6.4)	14.2	0.89 (t, 6.8)	14.3	0.84 (t, 6.4)
1''	20.3	2.00 (m)	73.2	4.20 (m)	19.9	2.18 (m)	25.4	1.38 (m)
2''	41.4	2.59 (m)	20.1	1.32 (m)	41.4	2.14, 2.46 (m)	31.9	2.36 (m)
3''	208.3		35.5	2.59 (m)	195.3		128.1	5.91 (br s)
4''	30.4		208.0		207.7		163.5	
5''		2.12 (s)	31.1	2.12 (s)	30.3	2.10 (s)	24.1	1.94 (s)
OH		11.52 (s)		11.46 (s)		11.11 (s)		

<sup>a</sup>Chemical shifts ( $\delta$ ) are in ppm. Coupling constants ( $J$ ) are in Hz.

**Table 2**Spectroscopic data for **1–4**

Compound	$[\alpha]_D^{25}$	CE at $n \rightarrow \pi^*$ carbonyl transition	$^1\text{H-NMR}$ for H-7	Absolute configuration at C-7
<b>1</b>	–	–	2.40	<i>S</i>
<b>2</b>	–	–	2.40	<i>S</i>
<b>3</b>	+	+	3.12	<i>R</i>
<b>4</b>	–	–	2.65	<i>S</i>

Table 3

Mosher ester analysis for 2

No	<sup>2</sup> δ <sub>H</sub> (CDCl <sub>3</sub> )	<sup>2</sup> δ <sub>H</sub> (py-d <sub>5</sub> )	(2 <i>S</i> )-ester δ <sub>H</sub> (py-d <sub>5</sub> )	(2 <i>R</i> )-ester δ <sub>H</sub> (py-d <sub>5</sub> )	Δδ <sub>H</sub> ( <i>SR</i> )
7	2.40	2.67	2.64	2.57	+0.07
1"	4.20	4.53	5.61	5.65	-0.04
2"	1.32	1.21	1.23	1.25	-0.02
9 <sub>ax</sub>	1.36	1.33	1.31	1.32	-0.01
10 <sub>eq</sub>	1.41	1.44	1.40	1.39	+0.01